

Three dimensional filamentary structures of a relativistic electron beam in Fast Ignition plasmas

Anupam Karmakar,* Naveen Kumar, and Alexander Pukhov
Institut für Theoretische Physik I, Heinrich-Heine-Universität, Düsseldorf, 40225, Germany

Oleg Polomarov and Gennady Shvets
*Department of Physics and Institute for Fusion Studies,
University of Texas at Austin, One University Station, Austin, TX 78712, USA*

The filamentary structures and associated electromagnetic fields of a relativistic electron beam have been studied by three dimensional particle-in-cell (PIC) simulations in the context of Fast Ignition fusion. The simulations explicitly include collisions in return plasma current and distinctly examine the effects of beam temperature and collisions on the growth of filamentary structures generated.

PACS numbers: 52.57.-z, 52.35.-g, 52.65.Rr

The transport of laser generated electron beams in overdense plasmas is an important topic to study specially in the context of Fast Ignition (FI)¹. PIC simulations and calculations have shown that the typical energy of electrons in these beams is of the order of a few MeV, which implies Giga-Ampere currents needed to transport Peta-Watt energy fluxes^{2,3}. However, the transportation of beam currents greater than the Alfvén current limit is not possible as the self-generated magnetic field associated with these currents bends electron trajectories strongly thereby preventing the forward propagation of the beam. In vacuum, the Alfvén current limit is $I_{alf} = 17\gamma\beta kA$, where $\gamma = 1/\sqrt{1-\beta^2}$ is the relativistic Lorentz factor associated with the beam. A current greater than this limit can only propagate as a charge neutralized current. This sort of situation occurs in the FI scenario, where the charge of the relativistic electron beam is compensated by the return plasma current and the propagation of the electron beam is possible. But this configuration, where two opposite streams of plasma currents are counterpropagating, is susceptible to the electrostatic two-stream instability and the transverse filamentation instability, often referred as the Weibel instability. Due to these instabilities, the electron beam gets splitted into many filaments^{4,5,6}. This filamentation can significantly affect the beam energy deposition at the center of the fuel target and thus is one of the central issues for the FI concept. Recently, Honrubia *et al.*⁷ have carried out 3D hybrid simulations of the fast electron transport and resistive beam filamentation in inertial fusion plasma. Califano *et al.*⁸ have reported three dimensional magnetic structures generated due to the Weibel instability of a relativistic electron beam in collisionless plasmas. Three dimensional PIC simulations of the Weibel instability in astrophysical context have also been reported⁹. Moreover, the evidence of Weibel-like dynamics and the resultant filamentation of electron beams have been observed experimentally¹⁰.

The role of collisions in the Weibel instability is rather non-trivial and has been studied analytically in linear and

quasilinear regime of the instability¹¹. The effect of collisions on the nonlinear regime of the instability is rather unaccessible to analytical calculations and can best be studied by PIC simulations. However, till now the full scale PIC simulations on the filamentation of the electron beams have mostly concentrated on the collisionless Weibel instability and have not explicitly included the effect of the collisions in the return plasma current. At the same time, collisions in the return plasma current play an important role on the Weibel instability. The eigenmodes of a collisional plasma have been computed recently, where it was shown that frictional nature of collisions can change the dynamics of the eigenmodes of the system significantly¹². In the presence of collisions the Weibel instability can not be suppressed by the transverse beam temperature as proposed initially¹³. A more focused discussion about the collisional effects on the Weibel instability has also been addressed recently where it was shown that even small collisions in the background plasma can trigger the Weibel instability of a warm electron beam that would be otherwise stable in collisionless plasma¹⁴.

Motivated by these findings, we carry out three-dimensional PIC simulations on the transport of a relativistic electron beam in the FI plasmas by explicitly including the effect of collisions in the return plasma current. The rationale behind choosing the 3D geometry is twofold: the first reason is to study the realistic geometry and the second is to show that in this geometry, the Weibel instability can't be suppressed due to the transverse beam temperature. It has been shown before analytically that in the 3D geometry the Weibel instability survives even with high transverse beam temperature due to the presence of an "oblique mode", which is the manifestation of coupling between the Weibel instability and the two-stream instability¹⁵. We conjecture the existence of the "oblique mode" due to the anomalous collisionality of the background plasma. It arises due to the turbulence of electrostatic fields generated by the two-stream instability. We choose four cases for the sim-

ulations (A) cold electron beam in a collisionless background plasma, (B) cold electron beam in a collisional background plasma, (C) warm electron beam in a cold collisionless background plasma, and (D) warm electron beam in a collisional background plasma, thus highlighting the influence of these physical processes separately. Hence, for the first time we have studied the filamentation of the relativistic beam investigating the role of each physical process clearly in three dimensional particle-in-cell simulations.

In our simulations, the electron beam propagates along the negative Z -axis with the relativistic velocity $v_{(b,z)} \gg v_{(b,x)}, v_{(b,y)}$. The bulk cold background plasma is represented by ambient plasma electrons, while the plasma ions are considered as a fixed charge-neutralizing background with the density $n_0 = n_b + n_p$, where n_b and n_p are the densities of the electron beam and the background plasma, respectively. Initially the beam current is fully compensated by the return plasma current. The beam density is much smaller than the background plasma electron density, *i.e.* $n_b \gg n_p$, a usual scenario of the FI. The spatial dimensions of the simulation domain L is large in comparison with the electron skin depth *i.e.* $L \gg \lambda_s$, where $\lambda_s = c/\omega_{pe}$; c and ω_{pe} are the velocity of light in vacuum and the total electron plasma frequency, respectively. The quasi-neutrality is maintained over all simulation time as the field evolutions due to the Weibel instability occur on a time scale slower than the plasma electron frequency $\Delta t \gg 1/\omega_{pe}$. The collisional processes are simulated with a newly implemented collision module in the relativistic PIC code Virtual Laser Plasma Laboratory (VLPL)¹⁶.

The 3D simulation box has spatial dimensions $X \times Y \times Z = (20\lambda_s \times 20\lambda_s \times 20\lambda_s)$. The 3D simulation domain is sampled with the mesh of $160 \times 80 \times 20$ cells. All simulations are performed with 64 particles per cell and with a grid size much smaller than the background plasma skin depth ($h_x, h_y, h_z \ll \lambda_s$). The density ratio between the beam and plasma electrons is $n_p/n_b = 9$, whereas the beam and the background plasma electrons have velocities $v_b = 0.9c$ and $v_p = 0.1c$. The evolution of the field energies for every component F_i of the fields \mathbf{E} and \mathbf{B} is recorded at every diagnostic step of the simulation summed over all the grid cells as

$$\int_V F_i^2 dx dy dz = \sum (eF_i m_e c \omega_{pe})^2 h_x h_y h_z, \quad (1)$$

where, h_x , h_y and h_z are the spatial grid sizes along x , y and z and $eF_i/m_e c \omega_{pe}$ represents the relativistic field normalizations. The relativistic electron beam has a temperature of $T_b \approx 70$ keV and the ambient plasma collision frequency is assumed to be $\nu_{ei}/\omega_{pe} = 0.15$ for these simulations. The background plasma is always cold initially while the beam electrons do not face any collisions.

Fig. 1 shows the structure of the beam filaments during the nonlinear regime at time $T = 16(2\pi/\omega_{pe})$ for the case (A). The filaments transverse spatial sizes are

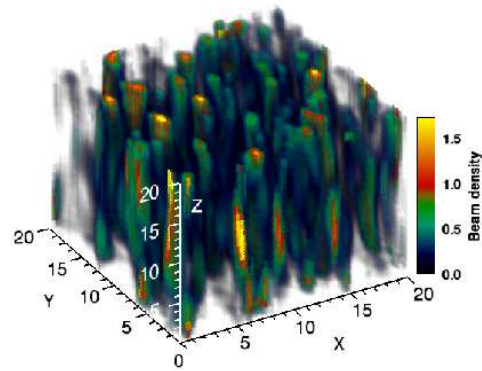


FIG. 1: (color online) 3D structure of the beam filaments generated in the PIC simulation at a time $T = 16(2\pi/\omega_{pe})$ in the nonlinear regime for the case (A), where the electron beam is cold and the plasma is collisionless. The filaments are tiny and their transverse dimension is comparable to the skin length of the cold background plasma.

comparable to the plasma skin depth λ_s while their longitudinal spatial extent is larger than the plasma skin depth. This could be understood as follows: in the linear regime of the beam filamentation, the transverse extent of the filaments is governed by the Weibel instability and its growth rate maximizes around the plasma skin depth in k -space. However, the longitudinal extent is determined by the two-stream instability which maximizes at wavelengths much larger than the plasma skin depth. As a result, the filaments have small spatial extent in the transverse direction and elongated in the propagation direction. Later on, during the nonlinear stage of the instability, the filaments merge together and their radii grow. The growth rate of the filamentation instability depends on the beam-to-plasma densities ratio, and is expressed as $\Gamma = (\sqrt{3}/2^{4/3}) (n_b/n_p \gamma_b)^{1/3}$, where γ_b is the relativistic Lorentz factor of the electron beam¹⁷. The Weibel instability generates very strong quasi-static magnetic field, which can be seen from the surface plot of the transverse (B_x, B_y) and longitudinal (B_z) magnetic field B_x shown in Fig. 2. Evidently, the amplitude of the transverse components is larger at least by one order of magnitude compared to the longitudinal component. The contour lines on the bottom surface in this figure show that each of these tiny filaments is surrounded by strong axial magnetic fields. We have plotted the temporal growth of such field energies for all four simulation cases later in Fig. 6.

The simulation case (B) is shown in Fig. 3. We observe that the transverse spatial width of the filaments is larger while the longitudinal extent remains unchanged. Due to collisions, the growth rate of the Weibel instability saturates at large plasma skin depth in k -space. At later times, the filaments merge together and their transverse spatial extent grows even larger, which is evident from the simulation results.

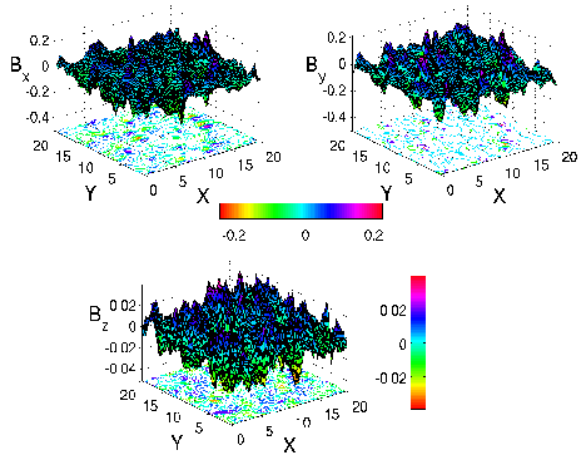


FIG. 2: (color online) Illustration of the transverse (B_x, B_y) and longitudinal (B_z) magnetic fields at the same time as Fig. 1. The contour lines on the bottom surface gives a 2D projection. \mathbf{B} fields are normalized as explained in the Eq. (1). Magnitude of the transverse components are larger almost by an order than the longitudinal component.

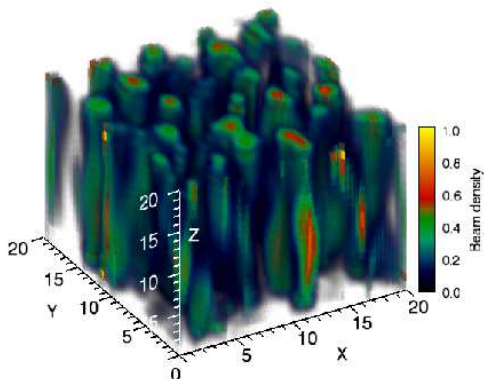


FIG. 3: (color online) 3D structure of the beam filaments from the PIC simulation in a time $T = 8(2\pi/\omega_{pe})$ for case (B), cold electron beam in collisional plasma. The filament sizes are larger than collisionless case due to collisional dissipation.

The filament structures of the simulation case (C), where the electron beam has a transverse beam temperature $T_b \approx 70$ keV, is shown in Fig. 4 at time $T = 10(2\pi/\omega_{pe})$. The Weibel instability could be suppressed by the high transverse beam temperature. However, in 3D geometry the coupling of the Weibel and the two-stream instabilities can manifest itself into the so called oblique mode, which persists even when the beam temperature is high. We may also consider the occurrence of the beam filamentation in this case due to “anomalous plasma collisionality” as shown in Ref.¹⁴. The two-stream mode actually generates electrostatic turbulence in the plasma. Stochastic fields associated with this tur-

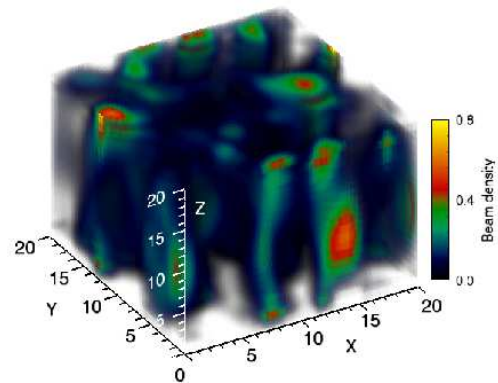


FIG. 4: (color online) Beam filamentation persists in the case (C), where the electron beam is warm with $T_b \approx 70$ keV propagating in a collisionless plasma, at time $T = 10(2\pi/\omega_{pe})$ in the nonlinear regime. The evacuation of the background plasma is not complete due to the strong thermal effects.

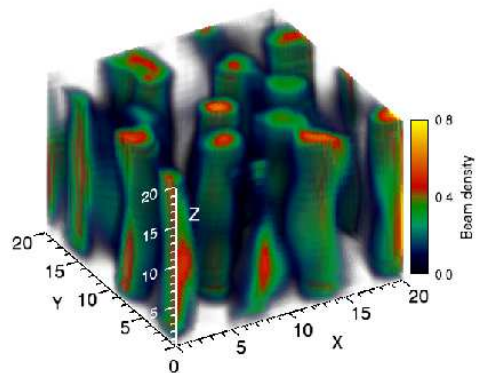


FIG. 5: Structure of the electron beam filaments derived from the PIC simulations for the case (D), where the warm electron beam is propagating in the collisional background plasma. The filaments are larger and total evacuation of the background plasma is prominent.

bulence scatter the beam and plasma electrons and lead to an effective collisionality in the return current. This anomalous effect revives back the Weibel instability. The phenomena of anomalous resistivity of plasma generated due to the turbulence of electric and magnetic fields have been noted earlier also³. The allowance for finite background plasma temperature decreases the growth rate of the instability. The interplay of collisions in different regimes of beam and background plasma temperatures on the Weibel instability can be found in Ref.¹¹. Moreover, it maybe worthwhile to mention here that this filamentation is lacking complete evacuation of the background plasma electrons contrary to the previous cases, presumably due to the strong thermal effects.

Fig. 5 shows the beam filaments of the last simulation

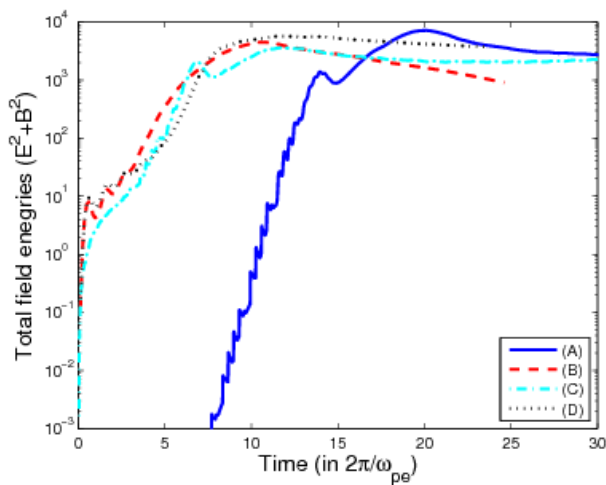


FIG. 6: (color online) Time evolution of Weibel field energies (E^2 and B^2) for the different simulation cases: (A) cold electron beam in a collisionless background plasma, (B) cold electron beam in a collisional background plasma, (C) hot electron beam in a collisionless plasma and (D) hot electron beam in collisional background plasma. The time is normalized in units of $2\pi/\omega_{pe}$ and the \mathbf{E} and \mathbf{B} fields are normalized as $(e\mathbf{E}/m_e\omega_{pe}c)$ and $(e\mathbf{B}/m_e\omega_{pe}c)$, respectively.

case (D), where the electron beam is hot and the background plasma is collisional. Here again we see strong filamentation and the spatial width of the beam filaments are also larger due to collective collisional plasma effects. Moreover, we have observed almost complete evacuation of the background plasma in this case.

To get further insight into the growth of the fields associated with the filamentation instability, we have studied the evolution of electric and magnetic field energies, shown in Fig. 6, for the four different simulation cases.

The vertical axes in Fig. 6 represents the normalized field energies in logarithmic scales whereas the horizontal axes are for time scaled in $2\pi/\omega_{pe}$. In each of these cases, we see a stage of linear instability, where the field energies build up exponentially in time and it is followed by the nonlinear saturation of the instability. Afterwards, in the nonlinear stage of the instability, the filaments merge rapidly with each other due to the magnetic attraction and the field energies saturate. One may note that the simulation cases (B), (C), and (D) display similar trend of field energy build up. This similarity is very interesting for the case (C), where the electron beam is warm and has the sufficiently high temperature to kill the Weibel instability. Yet, we still see the filamentation. Clearly it happens due to the presence of the two-stream or ‘‘oblique mode’’. Based on the similarity between cases (B) and (C), we attribute the filamentation of the beam to the ‘effective plasma collisionality’ of the beam system as discussed before in the manuscript as well¹⁴.

In summary, we have studied the filamentation instability of a relativistic electron beam in Fast Ignition plasma by three dimensional particle-in-cell simulations, distinctly examining the effects of high beam temperature and plasma collisions. The important result of this study is that the beam temperature does not suppress the filamentation instability even in absence of collisions in beam plasma system. An explanation on the persistence of the Weibel instability in 3D geometry is offered. It is attributed to the anomalous collisionality of the beam-plasma system due to the two-stream mode. The nonlinear regime of the filaments merging and the growth of field energies due to plasma collisions have been studied.

This work was supported by the DFG through TR-18 project and the US Department of Energy grants DE-FG02-04ER41321 and DE-FG02-04ER54763.

* Electronic address: anupam@tp1.uni-duesseldorf.de

¹ M. Tabak *et al.*, Phys. Plasmas **1**, 1626, (1994).

² A. Pukhov and J. Meyer-ter-Vehn, Phys. Rev. Lett. **76**, 3975 (1996), A. Pukhov and J. Meyer-ter-Vehn, Phys. Rev. Lett. **79**, 2686 (1997).

³ Y. Sentoku, K. Mima, P. Kaw and K. Nishikawa, Phys. Rev. Lett. **90**, 155001 (2003).

⁴ R. Lee and M. Lampe, Phys. Rev. Lett. **31**, 1390 (1973).

⁵ M. Honda, J. Meyer-ter-Vehn and A. Pukhov, Phys. Rev. Lett. **85**, 2128, (2000).

⁶ L. A. Cottrill *et al.* Phys. Plasmas, **15**, 082108 (2008).

⁷ J. J. Honrubia and J. Meyer-ter-Vehn, Nucl. Fusion, **46**, L-25 (2006).

⁸ F. Califano, D. Del Sarto and F. Pegoraro, Phys. Rev. Lett. **96**, 105008 (2006).

⁹ R. A. Fonseca, L. O. Silva, J. W. Tonge, W. B. Mori, and J. M. Dawson, Phys. Plasmas, **10**, 1979 (2003).

¹⁰ R. Jung *et al.*, Phys. Rev. Lett. **94**, 195001 (2005), M. Tatarakis *et al.* Phys. Rev. Lett. **90**, 175001 (2003), M. Wei *et al.* Phys. Rev. E **70**, 056412 (2004).

¹¹ C. Duetsch, A. Bret, M. C. Firpo and P. Fromy, Phys. Rev. E **72**, 026402 (2005), J. M. Wallace, J. U. Brackbill, C. W. Cranfill, D. W. Forslund, and R. J. Mason, Phys. Fluids **30**, 1085 (1987), M. Honda, Phys. Rev. E **69**, 016401 (2004), T. Okada and K. Niu, J. Plasma Phys. **23**, 423 (1980), **24**, 483 (1980), W. Kruer, S. Wilks, B. Lasinski, B. Langdon, R. Town, and M. Tabak, Bull. Am. Phys. Soc. **48**, 81 (2003).

¹² M. Honda, Phys. Rev. E, **69**, 016401 (2004).

¹³ L. O. Silva, R. A. Fonseca, J. W. Tonge, W. B. Mori, and J. M. Dawson, Phys. Plasmas, **9**, 2458, (2002).

¹⁴ A. Karmakar, N. Kumar, O. Polomarov, G. Shvets, and A. Pukhov, arXiv:0808.4078v2 [physics.plasm-ph] (under review in Phys. Rev. Lett.); A. Karmakar, N. Kumar, G. Shvets, and A. Pukhov (under review in Phys. Rev. E).

¹⁵ A. Bret, M.-C. Firpo and C. Deutsch, Phys. Rev. E **70**, 046401 (2004), Phys. Rev. Lett. **94**, 115002 (2005), Laser Part. Beams, **24**, 27 (2006), A. Bret, L. Grimmlet, D. Benisti and E. Lefebvre, Phys. Rev. Lett. **100**, 205008 (2008).

¹⁶ A. Pukhov, J. Plasma Phys. **61**, 425, (1999).

¹⁷ Ya. B. Fainberg, V. D. Shapiro, and V. I. Shevchenko, Sov.

Phys. JETP, **30**, 528 1970.